

Performance and Scalability of Voltage Controllers in Multi-Terminal HVDC Networks

Martin Andreasson, Emma Tegling, Henrik Sandberg and Karl H. Johansson

Abstract—In this paper, we compare the transient performance of a multi-terminal high-voltage DC (MTDC) grid equipped with a slack bus for voltage control to that of two distributed control schemes: a standard droop controller and a distributed averaging proportional-integral (DAPI) controller. We evaluate performance in terms of \mathcal{H}_2 metrics and show that the transient performance of a droop or DAPI controlled MTDC grid is always superior to that of an MTDC grid with a slack bus. In particular, we show that in the slack bus controlled network, the \mathcal{H}_2 norm that quantifies deviations from nominal voltage may grow unboundedly with network size, while it remains uniformly bounded with droop or DAPI control. We furthermore evaluate the resistive losses incurred in the voltage regulation transients, and show that these grow linearly in network size for all considered controllers, but are greatest in the slack bus case. We simulate the control strategies on radial MTDC networks to demonstrate that the transient performance for the slack bus controlled system deteriorates significantly as the network grows, which is not the case with the distributed control strategies.

I. INTRODUCTION

Transmitting power over long distances while maintaining low losses is one of the greatest challenges related to power transmission systems. Driven partly by increased deployment of renewable energy resources, such as large-scale off-shore wind farms, many distances between power generation and consumption are increasing. There is therefore a growing need for long-distance power transmission, motivating a widespread use of high-voltage direct current (HVDC) technology. Its higher investment costs compared to AC transmission lines are compensated by its lower resistive losses for sufficiently long distances, which are typically 500-800 km for overhead lines [1], but less than 100 km for undersea cable connections [2]. As more energy sources and consumers are connected by HVDC lines, the individual lines will eventually form a grid consisting of multiple terminals connected by several HVDC transmission lines, resulting in so-called multi-terminal HVDC (MTDC) systems [3].

The operation of MTDC transmission systems relies on the ability to control the DC voltages at the terminals; firstly, in order to govern the network's current flows, and secondly, in

order to avoid damage to power electronic equipment caused by too large deviations from nominal operating voltages [3], [4]. Different schemes for this voltage control in HVDC systems have been proposed in the literature. One method is to assign one of the buses (the *slack bus*) to control the networks' voltage drift through, e.g., a proportional-integral controller [5], [6]. Remaining buses control their injected currents according to Ohm's and Kirchhoff's laws [4]. We refer to this control strategy as *slack bus control*. The well-known *voltage droop controller*, on the other hand, is a decentralized proportional controller that regulates current injections based on local voltages [4], [5], [7]. This, however, typically leads to stationary voltage errors that can be eliminated through so-called secondary control. Several secondary controllers have been proposed in recent work [8]–[11]. Here, we focus on a distributed averaging proportional-integral (DAPI) controller.

The control problem aspects outlined above are relevant also for DC microgrids, which have spurred considerable research interest in recent years. DC microgrids are thought of as low-voltage distribution networks with distributed generation sources, storage elements and loads, all operating on DC [12], [13]. Although this paper will focus on HVDC systems, the same analysis can in principle be applied to DC microgrids, after a network reduction procedure laid out in [12].

The objective of this paper is to analyze the transient performance of the MTDC grid and to compare the slack bus control strategy to the voltage droop and the DAPI controllers. We evaluate performance through an \mathcal{H}_2 norm metric that quantifies expected voltage deviations over the voltage regulation transient. We show that the performance of a droop or DAPI controlled MTDC grid is always superior to that of a slack bus controlled grid. We also derive bounds on the scaling of the \mathcal{H}_2 norms with network size by studying systems built up on large-scale lattice networks. We find that, while the system's \mathcal{H}_2 norm remains bounded with droop or DAPI control for any network structure, that of a slack bus controlled system grows unboundedly with network size in 1- and 2-dimensional lattice networks. Our results therefore indicate that the slack bus control strategy is *not scalable* to larger networks, while droop and DAPI control are.

We also study a second transient performance metric and evaluate the resistive line losses that are associated with non-equilibrium power flows, caused by voltage fluctuations. This analysis builds on a recent series of work on AC power networks [14]–[16]. In line with those previous results, we

This work was supported in part by the European Commission, the Knut and Alice Wallenberg Foundation, by the Swedish Research Council through grant 2013-5523 and the Swedish Foundation for Strategic Research.

The authors are with the School of Electrical Engineering and the ACCESS Linnaeus Centre, KTH Royal Institute of Technology, SE-100 44 Stockholm, Sweden (mandreas, tegling, hsan, kallej@kth.se).

find that the total transient losses over the network grow linearly in the network size for all considered controllers, but are smallest with the DAPI controller.

The remainder of this paper is organized as follows. We introduce the MTDC network model, the voltage controllers, and the \mathcal{H}_2 performance metric in Section II. In Section III, we calculate the systems' \mathcal{H}_2 norms and continue to derive bounds on their scaling with network size in Section IV. Section V introduces and evaluates the transient resistive losses for the different controllers. We present a numerical simulation in Section VI and conclude in Section VII.

II. MODEL AND PROBLEM SETUP

A. Notation

Let $\mathcal{G} = (\mathcal{V}, \mathcal{E})$ be a graph, where $\mathcal{V} = \{1, \dots, n\}$ denotes the vertex set and $\mathcal{E} = \{1, \dots, m\}$ denotes the edge set. Let \mathcal{N}_i be the neighbor set of vertex $i \in \mathcal{V}$ in \mathcal{G} . For the MTDC network considered here, \mathcal{V} corresponds to the HVDC bus set, and \mathcal{E} corresponds to the set of HVDC lines. Throughout this paper, we assume that the graph underlying the MTDC network is connected. Denote by \mathcal{B} the vertex-edge adjacency matrix of a graph, and let $\mathcal{L}_W = \mathcal{B}W\mathcal{B}^T$ be its weighted Laplacian matrix, with edge-weights given by the elements of the positive definite diagonal matrix W . Let $c_{n \times m}$ be a matrix of dimension $n \times m$ whose elements are all equal to the number c , and c_n a column vector whose elements are all equal to c . Let $J_n = \frac{1}{n}1_{n \times n}$, and denote by A^* the conjugate transpose of the matrix A . For simplicity, we will often drop the time dependence of variables in the notation, e.g., $x(t)$ will be denoted x .

B. Model

Consider an MTDC transmission system consisting of n HVDC terminals, denoted by the vertex set $\mathcal{V} = \{1, \dots, n\}$. The DC terminals are connected by m HVDC transmission lines, denoted by the edge set $\mathcal{E} = \{1, \dots, m\}$. The HVDC lines are assumed to be purely resistive, neglecting capacitive and inductive elements of the HVDC lines. The assumption of purely resistive lines is not restrictive for the control applications considered in this paper, since line capacitance can be included in the capacitances of the terminals [4]. This implies that the current I_{ij} on the HVDC line from terminal i to terminal j is given by

$$I_{ij} = \frac{1}{R_{ij}}(V_i - V_j),$$

due to Ohm's law, where V_i is the voltage deviation from the nominal voltage V_i^{nom} of terminal i , and R_{ij} is the line resistance. The voltage dynamics of an arbitrary DC terminal i are assumed to be given by

$$C_i \dot{V}_i = - \sum_{j \in \mathcal{N}_i} I_{ij} + u_i = - \sum_{j \in \mathcal{N}_i} \frac{1}{R_{ij}}(V_i - V_j) + u_i, \quad (1)$$

where $C_i > 0$ is the total capacitance of terminal i , including that of the incident HVDC line as well as any shunt capacitances, and u_i is the controlled injected current for which

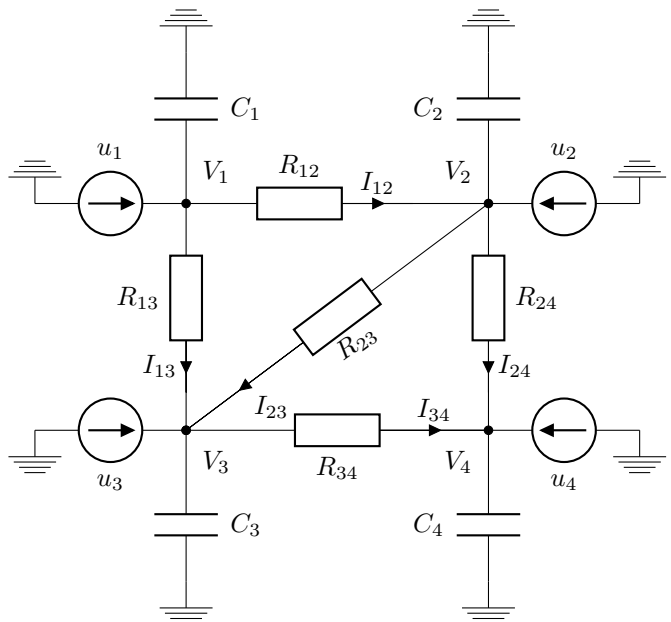


Fig. 1: Example of an MTDC network consisting of 4 terminals (buses) and 5 lines.

we will shortly introduce control schemes. In Fig. 1, a four terminal MTDC system is illustrated. Equation (1) may be written in vector-form as

$$C\dot{V} = -\mathcal{L}_R V + u, \quad (\mathcal{S}_{\text{MTDC}})$$

where $V = [V_1, \dots, V_n]^T$, $C = \text{diag}([C_1, \dots, C_n])$, $u = [u_1, \dots, u_n]^T$ and \mathcal{L}_R is the weighted Laplacian matrix of the graph representing the transmission lines, whose edge-weights are given by the conductances $\frac{1}{R_{ij}}$.

C. Slack bus control

A common control strategy for MTDC grids is to control the voltage at one terminal, by means of, e.g., a proportional-integral controller. This terminal, which then regulates the network's voltage drift, is called a slack bus. This control strategy can be idealized by assuming that the slack bus is grounded, that is,

$$V_1(t) = 0, \quad \forall t \geq 0, \quad (2)$$

where, without loss of generality, we have assigned terminal 1 to be the slack bus. This results in the following dynamics for the remaining buses

$$\tilde{C}\dot{\tilde{V}} = -\tilde{\mathcal{L}}_R \tilde{V}, \quad (\mathcal{S}_{\text{slack}})$$

where $\tilde{\mathcal{L}}_R$ is the reduced Laplacian matrix of \mathcal{L}_R , which is obtained by deleting the first row and the first column of \mathcal{L}_R , \tilde{C} is obtained mutatis mutandis, and $\tilde{V} = [V_2, \dots, V_n]^T$.

With slack bus control (also called constant DC voltage control), the network's operation relies on the functioning of one single terminal. Therefore, to increase the reliability of multi-terminal networks, distributed or decentralized control schemes inspired by frequency control in AC networks have been proposed [5], [6]. We next introduce two such controllers.

D. Droop control

The voltage droop controller is a commonly proposed method for controlling ($\mathcal{S}_{\text{MTDC}}$), see, e.g., [5], [12]. The droop controller, which is a decentralized proportional controller, takes the form

$$u = -K_P V, \quad (3)$$

where $K_P = \text{diag}\{K_{P_1}, \dots, K_{P_n}\}$ contains the droop gains $K_{P_i} > 0$. Inserting (3) in ($\mathcal{S}_{\text{MTDC}}$) yields the closed-loop system

$$C\dot{V} = -(\mathcal{L}_R + K_P)V. \quad (\mathcal{S}_{\text{droop}})$$

E. Distributed averaging proportional-integral (DAPI) control

Various secondary controllers have been proposed for MTDC grids and DC microgrids, with the objective to achieve current sharing and to eliminate static voltage errors [8]–[11]. Here, we consider a distributed averaging proportional-integral (DAPI) controller, which appends a secondary controller layer with an associated communication network to the droop controller ($\mathcal{S}_{\text{droop}}$). The DAPI controller has been successfully applied in frequency control of AC grids [17]–[20], and recently also for voltage control in AC grids [21]. A similar controller was also proposed in [12] in the context of DC microgrids. The DAPI controller can be written as

$$\begin{aligned} u &= -K_P V - z \\ K\dot{z} &= V - \mathcal{L}_q z, \end{aligned} \quad (4)$$

where \mathcal{L}_q is the Laplacian matrix of the connected graph describing the communication topology, and $K = \text{diag}\{K_1, \dots, K_n\}$ with the constant gains $K_i > 0$. Inserting (4) in ($\mathcal{S}_{\text{MTDC}}$) yields the closed-loop system

$$\begin{bmatrix} K\dot{z} \\ C\dot{V} \end{bmatrix} = \begin{bmatrix} -\mathcal{L}_q & I_n \\ -I_n & -(\mathcal{L}_R + K_P) \end{bmatrix} \begin{bmatrix} z \\ V \end{bmatrix}. \quad (\mathcal{S}_{\text{DAPI}})$$

F. Performance metric

We use an \mathcal{H}_2 norm metric to compare the performance of the proposed controllers for MTDC grids. Consider a general input-output stable linear MIMO system \mathcal{S} ,

$$\begin{aligned} \dot{x} &= Ax + Bw \\ y &= Hx, \end{aligned} \quad (\mathcal{S})$$

with transfer matrix $G(s) = H(sI_n - A)^{-1}B$. The (squared) \mathcal{H}_2 norm of \mathcal{S} is defined as

$$\|S\|_{\mathcal{H}_2}^2 \triangleq \frac{1}{2\pi} \int_{-\infty}^{\infty} \text{tr}(G(i\omega)^* G(i\omega)) d\omega.$$

The motivation for studying the \mathcal{H}_2 norm performance metrics for MTDC grids comes from two useful interpretations of the \mathcal{H}_2 norm (see also [15]):

- i) (Asymptotic covariance) If the input w is a white second order process with unit covariance (white noise), then

$$\|S\|_{\mathcal{H}_2}^2 = \lim_{t \rightarrow \infty} \text{E}\{y^*(t)y(t)\},$$

i.e., the (squared) \mathcal{H}_2 norm is the steady-state variance of the output components.

- ii) (Transient response) If the input $w \equiv 0_n$ and the initial value $x(0) = x_0$ is a random variable with covariance $\text{E}\{x_0 x_0^*\} = BB^*$, then

$$\|S\|_{\mathcal{H}_2}^2 = \int_0^{\infty} \text{E}\{y^*(t)y(t)\} dt,$$

i.e., the \mathcal{H}_2 norm is the expected \mathcal{L}_2 norm of the output y .

In the first part of this paper, we shall consider the following outputs when calculating the \mathcal{H}_2 norm:

$$y = \frac{1}{\sqrt{n}} V \quad (5)$$

for ($\mathcal{S}_{\text{droop}}$) and ($\mathcal{S}_{\text{DAPI}}$), and

$$y = \frac{1}{\sqrt{n}} \tilde{V} \quad (6)$$

for ($\mathcal{S}_{\text{slack}}$). In other words, performance will be evaluated in terms of the mean (per node) deviation from nominal voltage in the case of i) a persistent stochastic disturbance input w due to e.g. fluctuating load currents, or ii) random initial voltage perturbations that, since we can assume $B = I_n$, are uncorrelated across nodes.

III. \mathcal{H}_2 NORM EVALUATION

In this section, we compute the \mathcal{H}_2 norm of the closed-loop dynamics ($\mathcal{S}_{\text{slack}}$), ($\mathcal{S}_{\text{droop}}$), and ($\mathcal{S}_{\text{DAPI}}$). In order to provide tractable closed-form expressions for the \mathcal{H}_2 norms, we impose the following assumptions, which will be assumed to hold henceforth.

Assumption 1 (Uniform system parameters). *The capacitances C_i and the gains K_{P_i} and K_i are uniform across the network and given by the positive constants c , k_P and k , respectively.*

Assumption 2 (Communication graph). *The Laplacian matrix \mathcal{L}_q of the communication graph used by the DAPI controller in ($\mathcal{S}_{\text{DAPI}}$) satisfies $\mathcal{L}_q = \gamma \mathcal{L}_R$, $\gamma > 0$, where \mathcal{L}_R was defined in ($\mathcal{S}_{\text{MTDC}}$).*

The following theorem summarizes the main result of this section.

Theorem 1 (Performance evaluation). *Let Assumptions 1 and 2 hold. The performance of the slack bus controlled MTDC grid ($\mathcal{S}_{\text{slack}}$) with output (6) is given by*

$$\|\mathcal{S}_{\text{slack}}\|_{\mathcal{H}_2}^2 = \frac{c}{2n} \sum_{i=1}^{n-1} \frac{1}{\tilde{\lambda}_i}, \quad (7)$$

where $\tilde{\lambda}_i$ denotes the i^{th} eigenvalue of the reduced Laplacian $\tilde{\mathcal{L}}_R$. The performance of the droop-controlled MTDC grid ($\mathcal{S}_{\text{droop}}$) with output (5) is given by

$$\|\mathcal{S}_{\text{droop}}\|_{\mathcal{H}_2}^2 = \frac{c}{2n} \sum_{i=1}^n \frac{1}{(\lambda_i + k_P)}, \quad (8)$$

where λ_i denotes the i^{th} eigenvalue of \mathcal{L}_R . The performance of the DAPI controlled MTDC grid ($\mathcal{S}_{\text{DAPI}}$) with output (5) is given by

$$\|\mathcal{S}_{\text{DAPI}}\|_{\mathcal{H}_2}^2 = \frac{c}{2n} \sum_{i=1}^n \frac{1}{\left(\lambda_i + k_P + \frac{c\gamma\lambda_i}{c\gamma^2\lambda_i^2 + k\gamma\lambda_i^2 + k k_P \gamma \lambda_i + k}\right)}. \quad (9)$$

Proof: It is readily verified that the system matrices of the systems ($\mathcal{S}_{\text{slack}}$), ($\mathcal{S}_{\text{droop}}$), ($\mathcal{S}_{\text{DAPI}}$) are Hurwitz if $c, k, k_P, \gamma > 0$ (noting that the grounded Laplacian $\tilde{\mathcal{L}}_R$ is positive definite if the graph \mathcal{G} is connected, see [15]). Therefore, their \mathcal{H}_2 norms exist and are finite. To derive the respective norms, we follow the procedure outlined in [14] and perform a unitary state transformation, which in the case of ($\mathcal{S}_{\text{droop}}$) reads $V = U\bar{V}$. The matrix U diagonalizes \mathcal{L}_R , i.e., $\mathcal{L}_R = U^*\Lambda U$ with $\Lambda = \text{diag}(\lambda_1, \dots, \lambda_n)$. Since the \mathcal{H}_2 norm is unitarily invariant, we can also define $\bar{y} = U^*y$ and $\bar{w} = U^*w$ and obtain, in the new coordinates,

$$\begin{aligned} c\dot{\bar{V}} &= -(\Lambda + k_P I_n)\bar{V} + \bar{w} \\ \bar{y} &= \frac{1}{\sqrt{n}}\bar{V}. \end{aligned} \quad (10)$$

The system (10) now consists of n decoupled subsystems ($\mathcal{S}_{\text{droop}}^i$):

$$\begin{aligned} \dot{\bar{V}}_i &= -\frac{1}{c}(\lambda_i + k_P)\bar{V}_i + \frac{1}{c}\bar{w}_i \triangleq \bar{A}_{\text{droop}}^i \bar{V}_i + \bar{B}^i \bar{w}_i \\ \bar{y}_i &= \frac{1}{\sqrt{n}}\bar{V}_i \triangleq \bar{H}^i \bar{V}_i, \end{aligned} \quad (11)$$

and it holds that $\|\mathcal{S}_{\text{droop}}\|_{\mathcal{H}_2}^2 = \sum_{i=1}^n \|\mathcal{S}_{\text{droop}}^i\|_{\mathcal{H}_2}^2$. Each individual subsystem norm can now be evaluated by solving the Lyapunov equation for P^i :

$$\bar{A}_{\text{droop}}^{i*} P^i + P^i \bar{A}_{\text{droop}}^i = -\bar{H}^{i*} \bar{H}^i,$$

and taking $\|\mathcal{S}_{\text{droop}}^i\|_{\mathcal{H}_2}^2 = \text{tr}(\bar{B}^{i*} P^i \bar{B}^i)$, which in our case gives

$$\|\mathcal{S}_{\text{droop}}^i\|_{\mathcal{H}_2}^2 = \frac{c}{2n(\lambda_i + k_P)}. \quad (12)$$

Summing over the n subsystems yields the result in (8).

The \mathcal{H}_2 norms of ($\mathcal{S}_{\text{slack}}$) and ($\mathcal{S}_{\text{DAPI}}$) are calculated in a similar manner. \blacksquare

Next, we show that the \mathcal{H}_2 norm of ($\mathcal{S}_{\text{DAPI}}$) is strictly smaller than that of ($\mathcal{S}_{\text{droop}}$), which in turn is strictly smaller than that of ($\mathcal{S}_{\text{slack}}$).

Corollary 2. *For any choice of the parameters $c, k, k_P, \gamma > 0$, it holds that*

$$\|\mathcal{S}_{\text{DAPI}}\|_{\mathcal{H}_2}^2 < \|\mathcal{S}_{\text{droop}}\|_{\mathcal{H}_2}^2 < \|\mathcal{S}_{\text{slack}}\|_{\mathcal{H}_2}^2.$$

Proof: By Cauchy's interlacing theorem [22], the eigenvalues λ_i of \mathcal{L}_R and the eigenvalues $\tilde{\lambda}_i$ of $\tilde{\mathcal{L}}_R$ satisfy

$$0 = \lambda_1 < \tilde{\lambda}_1 \leq \lambda_2 \leq \dots \leq \tilde{\lambda}_{n-1} \leq \lambda_n.$$

Thus

$$\sum_{i=1}^{n-1} \frac{c}{2n\lambda_i} \geq \sum_{i=2}^n \frac{c}{2n\lambda_i} > \sum_{i=1}^n \frac{c}{2n(\lambda_i + k_P)},$$

which proves the second inequality. Furthermore, since $c, k, k_P, \gamma, \lambda_i > 0$, each term in the sum in (9) is smaller than the corresponding term in (8), so $\|\mathcal{S}_{\text{DAPI}}\|_{\mathcal{H}_2}^2 < \|\mathcal{S}_{\text{droop}}\|_{\mathcal{H}_2}^2$, which concludes the proof. \blacksquare

IV. PERFORMANCE SCALING IN LATTICE NETWORKS

By Corollary 2 we know that the \mathcal{H}_2 norms of the droop or DAPI controlled MTDC grids are always smaller than that of the slack bus controlled grid. It turns out, as we will show in this section, that this difference in performance becomes increasingly pronounced as the network size grows. In particular, for specific network topologies, we show that the \mathcal{H}_2 norm of the slack bus controlled MTDC network may grow unboundedly with network size, while it remains bounded with droop or DAPI control. This scaling of performance with network size becomes a particularly important question as DC microgrids are gaining interest, since these are likely to comprise a greater number of buses than MTDC grids for high voltage applications.

In order to derive the relevant performance bounds, we first make the physically motivated assumption that the resistances in the grid are uniformly bounded.

Assumption 3 (Uniformly bounded resistances). *The network line resistances are uniformly bounded as*

$$\underline{R} \leq R_{ij} \leq \bar{R}, \quad (i, j) \in \mathcal{E},$$

where \underline{R} and \bar{R} are positive constants.

Recall that the \mathcal{H}_2 norm of the slack bus controlled MTDC grid is given by

$$\|\mathcal{S}_{\text{slack}}\|_{\mathcal{H}_2}^2 = \frac{c}{2n} \sum_{i=1}^{n-1} \frac{1}{\lambda_i} \geq \frac{c}{2n} \sum_{i=2}^n \frac{1}{\lambda_i}. \quad (13)$$

Here, λ_i are the eigenvalues of the graph Laplacian \mathcal{L}_R , and we notice immediately that this expression grows large if one or more of the eigenvalues approaches zero. This is typically the case, unless the network is well-interconnected. More precisely, the scaling of performance will depend on how

$$K^* \triangleq \frac{1}{n} \sum_{i=2}^n \frac{1}{\lambda_i} \quad (14)$$

scales with network size. The quantity K^* is closely related to the *Kirchhoff index*, also called total effective resistance or Wiener index, in resistor networks. Namely, given a network of resistors, define the pairwise effective resistance between two nodes i and j as R_{ij}^{eff} . The Kirchhoff index is defined as

$$K_f \triangleq \sum_{i < j} R_{ij}^{\text{eff}}, \quad (15)$$

see, e.g., [23], [24]. The Kirchhoff index has been shown in [25] to equal:

$$K_f = n \sum_{i=2}^n \frac{1}{\lambda_i}.$$

Clearly $K^* = \frac{K_f}{n^2}$, so $K^* \rightarrow \infty$ if and only if $\frac{K_f}{n^2} \rightarrow \infty$ as $n \rightarrow \infty$. The following intuitive result proves to be very useful for our analysis.

Lemma 3 (Rayleighs monotonicity law). *Removing an edge from a graph, or increasing its resistance, can only increase the effective resistance between any two points in the network. Conversely, adding edges or decreasing their resistance can only decrease the effective resistance between any two points.*

Proof: See, e.g., [26]. ■

Rayleighs monotonicity law implies that well-interconnected networks have a lower Kirchhoff index, and hence a lower \mathcal{H}_2 norm (better performance) than sparsely interconnected networks. It also implies that the Kirchhoff index of any network that can be *embedded* in a larger network (that is a subgraph of the larger network) is at least as large as that of the larger network [27].

We will next consider a subclass of graphs for which asymptotic (in network size) bounds on the Kirchhoff index K_f can be obtained analytically, namely infinite lattices and their fuzzes, which are defined below.

Definition 1 (Lattice). *A d -dimensional lattice is a graph that has a node at every point in \mathbb{Z}^d and an edge between two nodes if and only if the Euclidean distance between the nodes is 1.*

Definition 2 (h -fuzz). *The h -fuzz of a lattice is obtained by adding an edge between any nodes within distance h .*

By the reasoning above, the Kirchhoff index, and thereby the performance scaling, derived for lattices and fuzzes provides a lower bound for all graphs that can be embedded in them. In this context, it is useful to think of the spatial dimension d as a measure of the graph's connectivity, which determines how performance scales in the network. Consider the following theorem:

Theorem 4 (Asymptotic performance in lattices). *Let the graph \mathcal{G} corresponding to the MTDC network be a lattice or its h -fuzz in d dimensions. Then, under Assumptions 1–3, the asymptotic scaling of performance in the slack bus controlled MTDC network is given in Table I. This implies that for 1- and 2-dimensional lattices and h -fuzzes, the \mathcal{H}_2 norm of the slack bus controlled network scales as n and $\log(n)$, respectively, and thus grows unboundedly as $n \rightarrow \infty$.*

The \mathcal{H}_2 norms of droop and DAPI controlled MTDC networks are, on the other hand, upper bounded by

$$\begin{aligned} \|S_{\text{droop}}\|_{\mathcal{H}_2}^2 &\leq \frac{c}{2k_P} \\ \|S_{\text{DAPI}}\|_{\mathcal{H}_2}^2 &\leq \frac{c}{2k_P}, \end{aligned}$$

for any underlying network structure (that is, not limited to lattices and fuzzes).

Proof: In order to bound the \mathcal{H}_2 norm of the slack bus controlled system, by (13) it suffices to bound the quantity $\sum_{i=2}^n \frac{c}{2n\lambda_i} = \frac{1}{2n^2} K_f$. Note that, by Assumption 3, the network's resistances are upper and lower bounded. Consider

TABLE I: Performance scaling of the slack bus controlled MTDC network on lattices and h -fuzzes, as the network size $n \rightarrow \infty$, where a_1, a_2 are positive constants.

Lattice dimension	\mathcal{H}_2 norm, slack bus
$d = 1$	$a_1 n \leq \ S_{\text{slack}}\ _{\mathcal{H}_2}^2$
$d = 2$	$a_2 \log(n) \leq \ S_{\text{slack}}\ _{\mathcal{H}_2}^2$

therefore the graphs where the resistances R_{ij} are replaced by their lower and upper bounds. By Lemma 3, the Kirchhoff indices of these graphs bound the Kirchhoff index of the original graph. Now, by [27] the effective resistance between any two points i and j can be bounded as

$$\begin{aligned} \alpha_1 d_G(i, j) &\leq R_{ij}^{\text{eff}} \leq \beta_1 d_G(i, j) \\ \alpha_2 \log(d_G(i, j)) &\leq R_{ij}^{\text{eff}} \leq \beta_2 \log(d_G(i, j)) \\ \alpha_3 &\leq R_{ij}^{\text{eff}} \leq \beta_3, \end{aligned}$$

for, respectively, the 1, 2 and 3-dimensional lattice or fuzz with uniform resistances. Here, the α 's and β 's are positive constants, which depend on \underline{R} and \bar{R} , but are independent of n . The function $d_G(i, j)$ denotes the graph distance between nodes i and j , which is equal to the ℓ_1 -norm between i and j .

For $d = 1$, the graph distance between two arbitrary nodes in a lattice with n nodes, is proportional to n [27]. Summing over all $i \leq j$ as in (15) yields $\alpha'_1 n^3 \leq K_f \leq \beta'_1 n^3 \Leftrightarrow \alpha'_1 n \leq K^* \leq \beta'_1 n$, for some constants α'_1, β'_1 . Based on (13), the \mathcal{H}_2 norm can then be lower bounded as in Table I.

For $d = 2$, the graph distance between two arbitrary nodes in a lattice with n nodes, scales as \sqrt{n} . Summing over $i \leq j$ yields $\alpha'_2 n^2 \log(n) \leq K_f \leq \beta'_2 n^2 \log(n) \Leftrightarrow \alpha'_2 \log(n) \leq K^* \leq \beta'_2 \log(n)$ for some α'_2, β'_2 . The lower bound of the \mathcal{H}_2 norm can then be stated as in Table I.

For $d = 3$, R_{ij} is bounded by positive constants, so summing over $i \leq j$ yields $\alpha'_3 n^2 \leq K_f \leq \beta'_3 n^2 \Leftrightarrow \alpha'_3 \leq K^* \leq \beta'_3$, that is, the \mathcal{H}_2 norm is bounded.

Next, it is straightforward to show that $\|S_{\text{droop}}\|_{\mathcal{H}_2}^2$ and $\|S_{\text{DAPI}}\|_{\mathcal{H}_2}^2$ are upper bounded by $\frac{c}{2k_P}$, regardless of the λ_i , that is, of the network structure. ■

Theorem 4 implies that, unless the network is well-interconnected, controlling the voltage of large MTDC grids by means of a slack bus may be unsuitable, as the \mathcal{H}_2 norm may scale unboundedly with the network size. As a result, one would obtain growing expected deviations from desired voltage levels. The \mathcal{H}_2 norms of the droop or DAPI controlled MTDC grids, on the other hand, are always uniformly upper bounded with respect to the network size, regardless of the network topology, making droop and DAPI control more *scalable* control strategies.

Similar analyses as the above have been carried for AC power grids and coupled oscillator networks in [16], [28], [29]. However, our results for the MTDC grids partly differ from those derived for AC grids, as the droop controller alone suffices to uniformly bound the \mathcal{H}_2 norm, whereas

a DAPI controller is required in AC grids. This can be understood by studying the control law ($\mathcal{S}_{\text{droop}}$) and noting that the diagonal matrix K_P enables *absolute* feedback from the voltage deviations, i.e., a type of *self-damping*. Such absolute feedback has been shown in [30] to be key in achieving boundedness in \mathcal{H}_2 norm scalings of this type. For AC networks, on the other hand, absolute feedback from phase angles is not present in the droop control law, but can be emulated by the DAPI controller [16].

V. TRANSIENT RESISTIVE LOSSES

We now shift focus to a different performance metric, and consider the resistive power losses incurred in the power lines as the system is returning to desired voltage levels after a disturbance. In AC power grids, such transient losses, associated with phase synchronization, have recently been found to scale linearly with the network size, and, unlike the performance metric considered in Sections III–IV, not to decrease with increasing network connectivity [14]–[16].

In order to explore the transient losses in MTDC grids, consider the power loss in the HVDC line connecting buses i and j , which is given by

$$P_{ij}^{\text{loss}} = \frac{1}{R_{ij}}(V_i - V_j)^2.$$

Summing over all network lines yields

$$P^{\text{loss}} = \sum_{(i,j) \in \mathcal{E}} P_{ij}^{\text{loss}} = \sum_{(i,j) \in \mathcal{E}} \frac{1}{R_{ij}}(V_i - V_j)^2 = V^T \mathcal{L}_R V.$$

Therefore, the total resistive energy losses in the power lines in an MTDC grid will be given by:

$$E^{\text{loss}} = \int_0^\infty P^{\text{loss}} dt = \int_0^\infty V^T(t) \mathcal{L}_R V(t) dt. \quad (16)$$

Now, if the initial value $V(0)$ is zero mean Gaussian and uncorrelated across the network nodes, then the *expected value* of E^{loss} over the transient equals the squared \mathcal{H}_2 norm of the underlying dynamical system with output given by $y = \mathcal{L}_R^{1/2} V$ (see [15] for a more thorough discussion). Thus the same techniques used in Section III can be used to calculate the expected transient energy losses here. We characterize those losses in the following theorem.

Theorem 5 (Transient resistive losses). *Let Assumptions 1 and 2 hold, and let $V(0)$ be zero mean Gaussian with correlation $\mathbb{E}\{V(0)V(0)^T\} = I_n$. The expected transient resistive losses of the slack bus controlled MTDC grid ($\mathcal{S}_{\text{slack}}$) are then given by*

$$E_{\text{slack}}^{\text{loss}} = \frac{c}{2}(n-1). \quad (17)$$

The corresponding losses of the droop controlled MTDC grid ($\mathcal{S}_{\text{droop}}$) are given by

$$E_{\text{droop}}^{\text{loss}} = \frac{c}{2} \sum_{i=2}^n \frac{\lambda_i}{\lambda_i + k_P}, \quad (18)$$

and those of the DAPI controlled MTDC grid ($\mathcal{S}_{\text{DAPI}}$) are given by

$$E_{\text{DAPI}}^{\text{loss}} = \frac{c}{2} \sum_{i=2}^n \frac{\lambda_i}{\lambda_i + k_P + \frac{c\gamma\lambda_i}{c\gamma^2\lambda_i^2 + k\gamma\lambda_i^2 + k k_P \gamma \lambda_i + k}}. \quad (19)$$

Proof: The expected transient resistive losses $E_{\text{droop}}^{\text{loss}}$ and $E_{\text{DAPI}}^{\text{loss}}$ are given by the \mathcal{H}_2 norms of ($\mathcal{S}_{\text{droop}}$) and ($\mathcal{S}_{\text{DAPI}}$) with the output $y = \mathcal{L}_R^{1/2} V$. Since this output equation is also diagonalizable by the unitary matrix U that diagonalized \mathcal{L}_R , the \mathcal{H}_2 norms can be calculated in analogy to the proof of Theorem 1.

For the slack bus controlled MTDC grid, recall first that bus 1 is the slack bus, so that $V_1 \equiv 0$ by design. Consider the energy function

$$W = \frac{1}{2} V^T C V,$$

and note that since ($\mathcal{S}_{\text{slack}}$) is asymptotically stable, $W \rightarrow 0$ as $t \rightarrow \infty$. Define

$$\tilde{\mathcal{L}}_R = \begin{bmatrix} 0 & 0_n^T \\ 0_n & \tilde{\mathcal{L}}_R \end{bmatrix},$$

where $\tilde{\mathcal{L}}_R$ is the reduced Laplacian. Now, consider the time derivative of W

$$\dot{W} = V^T C \dot{V} = -V^T \tilde{\mathcal{L}}_R V = -V^T \mathcal{L}_R V,$$

where we have used the dynamics in ($\mathcal{S}_{\text{slack}}$) and that $V_1 = 0$. Integrating the above equation and keeping in mind that $W \rightarrow 0$ as $t \rightarrow \infty$, we obtain

$$\begin{aligned} E_{\text{slack}}^{\text{loss}} &= \int_0^\infty V^T(t) \mathcal{L}_R V(t) dt \\ &= \frac{1}{2} V^T(0) C V(0) = \frac{c}{2} \tilde{V}^T(0) \tilde{V}(0), \end{aligned}$$

since $C = cI_n$ by Assumption 1. Now, $\tilde{V}(0)$ is, just as $V(0)$, zero mean Gaussian with unit variance by assumption, so $\mathbb{E}\{\tilde{V}^T(0)\tilde{V}(0)\} = n-1$ and the result in (17) follows. ■

As was the case with Corollary 2, the following corollary follows from Theorem 5:

Corollary 6. *For any choice of the parameters $c, k, k_P, \gamma > 0$, it holds that*

$$E_{\text{DAPI}}^{\text{loss}} < E_{\text{droop}}^{\text{loss}} < E_{\text{slack}}^{\text{loss}},$$

that is, the slack bus controller has the worst performance in terms of transient resistive losses.

With all considered controllers, the total transient resistive losses in Theorem 5 grow linearly with the number of buses. This resembles the situation in AC power grids, where losses have been found to grow linearly with the number of generator buses. If evaluated *per bus*, the resistive losses are hence uniformly bounded for all considered controllers, also as the network size grows large. Perhaps surprisingly, this holds in particular for an MTDC grid controlled by a slack bus, even though its \mathcal{H}_2 norm with respect to the performance output (6) grows unbounded with network size. Intuitively,

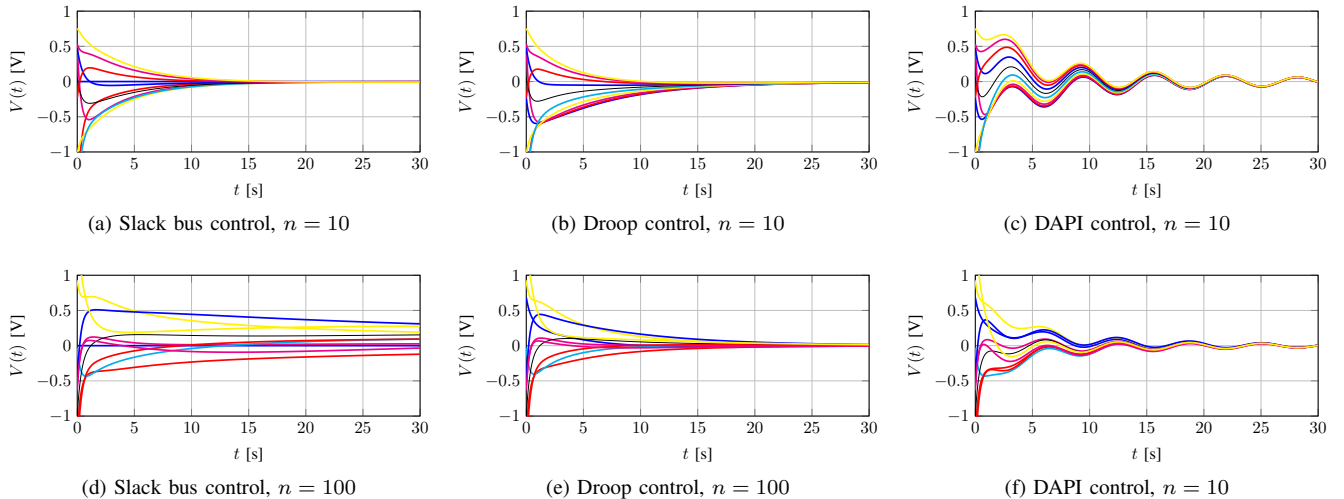


Fig. 2: Voltage trajectories (deviations from nominal voltage) for a subset of the buses in a radial MTDC network (1-dimensional lattice) of size $n = 10$ and $n = 100$ with, respectively, slack bus, droop, and DAPI control. In the slack bus case, we notice that performance deteriorates substantially for the larger network (d) compared to the smaller (a), which is not in the case with droop or DAPI control; compare (b–c) to (e–f). The oscillatory behavior in the DAPI case can be attributed to typical properties of integral control.

however, the resistive losses are always upper bounded by the initial energy of the system, which on expectation grows linearly in the number of buses for Gaussian initial conditions. Therefore, even though the slack bus controlled MTDC grid may converge slowly for certain network topologies as found in Section IV, the resistive losses during the transient only grow linearly in the number of buses. In droop and DAPI controlled MTDC grids on the other hand, the energy dissipated in the controllers contribute to the lower resistive losses in the network lines over the transient.

VI. SIMULATIONS

In this section, we demonstrate an implication of the performance scaling in Theorem 4 by a simulation of a radial MTDC grid (that is, a topology corresponding to a 1-dimensional lattice) with sizes $n = 10$ and $n = 100$. For simplicity, we let the resistances of all DC lines be 1Ω , and the capacitances of the DC buses be 1 mF . The controller parameters were set to $k_P = 0.1$, $k = 100$ and $\gamma = 1000$, respectively. The system was initiated at the voltage $V(0) = V_0$, where $V_0 \sim \mathcal{N}(0, 1)$.

The responses of the MTDC grid with the different controllers are shown in Fig. 2. From the figures, it is evident that the performance of the MTDC grid with a slack bus deteriorates significantly with increasing network size, while the performance of the droop and DAPI controlled MTDC grids remains almost unchanged as the network size increases.

VII. SUMMARY AND CONCLUSIONS

We quantified transient performance in MTDC networks using the \mathcal{H}_2 norm, which can be interpreted as the expected per bus \mathcal{L}_2 norm of the total voltage deviations under Gaussian initial conditions. The performance of an MTDC

grid controlled by means of a slack bus whose voltage is kept constant, is shown to be worse than that of a droop controlled grid. We showed that performance can be further improved by a DAPI controller. For network topologies resembling one- or two-dimensional lattices, the \mathcal{H}_2 norm scales unfavorably and grows unboundedly with the number of buses. On the other hand, the \mathcal{H}_2 norms of MTDC grids controlled with droop or DAPI controllers are always uniformly bounded with respect to the network size, regardless of topology. These control laws are therefore scalable, and thus amenable to larger MTDC grids.

We also evaluated the transient resistive losses in the HVDC lines, i.e., the total energy dissipated due to resistive line losses as voltages are regulated to their nominal values. Here too, the slack bus control displayed the worst performance. Even though the total resistive losses grow linearly with the number of buses for all controllers, they will, in contrast to the other \mathcal{H}_2 performance metric considered here, remain uniformly bounded when evaluated per bus.

REFERENCES

- [1] K. R. Padiyar, *HVDC power transmission systems: technology and system interactions*. New Delhi: New Age International, 1990.
- [2] P. Bresesti, W. L. Kling, R. L. Hendriks, and R. Vailati, "HVDC connection of offshore wind farms to the transmission system," *IEEE Transactions on Energy Conversion*, vol. 22, no. 1, pp. 37–43, 2007.
- [3] D. Van Hertem and M. Ghandhari, "Multi-terminal VSC HVDC for the european supergrid: Obstacles," *Renewable and Sustainable Energy Reviews*, vol. 14, no. 9, pp. 3156–3163, 2010.
- [4] P. Kundur, *Power System Stability and Control*. The EPRI Power System Engineering, New York: McGraw-Hill Companies, Inc., 1994.
- [5] T. M. Haileselassie and K. Uhlen, "Impact of DC line voltage drops on power flow of MTDC using droop control," *IEEE Transactions on Power Systems*, vol. 27, pp. 1441–1449, Aug 2012.
- [6] W. Wang and M. Barnes, "Power flow algorithms for multi-terminal VSC-HVDC with droop control," *IEEE Transactions on Power Systems*, vol. 29, pp. 1721–1730, July 2014.

- [7] P. Karlsson and J. Svensson, "DC bus voltage control for a distributed power system," *IEEE Transactions on Power Electronics*, vol. 18, pp. 1405 – 1412, nov. 2003.
- [8] A. Sarlette, J. Dai, Y. Phulpin, and D. Ernst, "Cooperative frequency control with a multi-terminal high-voltage DC network," *Automatica*, vol. 48, no. 12, pp. 3128 – 3134, 2012.
- [9] S. Anand, B. G. Fernandes, and M. Guerrero, "Distributed control to ensure proportional load sharing and improve voltage regulation in low-voltage DC microgrids," *Power Electronics, IEEE Transactions on*, vol. 28, pp. 1900–1913, April 2013.
- [10] X. Lu, J. Guerrero, K. Sun, and J. Vasquez, "An improved droop control method for DC microgrids based on low bandwidth communication with DC bus voltage restoration and enhanced current sharing accuracy," *IEEE Transactions on Power Electronics*, vol. 29, pp. 1800–1812, April 2014.
- [11] M. Andreasson, D. V. Dimarogonas, and K. H. Johansson, "Distributed controllers for multi-terminal HVDC transmission systems," *arXiv:1411.1864*, 2014.
- [12] J. Zhao and F. Dörfler, "Distributed control and optimization in DC microgrids," *Automatica*, vol. 61, pp. 18 – 26, 2015.
- [13] A. T. Elsayed, A. A. Mohamed, and O. A. Mohammed, "DC microgrids and distribution systems: An overview," *Electric Power Systems Research*, vol. 119, pp. 407 – 417, 2015.
- [14] B. Bamieh and D. F. Gayme, "The price of synchrony: Resistive losses due to phase synchronization in power networks," in *2013 American Control Conference*, pp. 5815–5820, June 2013.
- [15] E. Tegling, B. Bamieh, and D. F. Gayme, "The price of synchrony: Evaluating the resistive losses in synchronizing power networks," *IEEE Transactions on Control of Network Systems*, vol. 2, pp. 254–266, Sept 2015.
- [16] E. Tegling, M. Andreasson, J. W. Simpson-Porco, and H. Sandberg, "Improving performance of droop-controlled microgrids through distributed PI-control," in *American Control Conference*, July 2016.
- [17] J. W. Simpson-Porco, F. Dörfler, and F. Bullo, "Synchronization and power sharing for droop-controlled inverters in islanded microgrids," *Automatica*, vol. 49, no. 9, pp. 2603 – 2611, 2013.
- [18] M. Andreasson, D. Dimarogonas, K. H. Johansson, and H. Sandberg, "Distributed vs. centralized power systems frequency control," in *European Control Conference*, pp. 3524–3529, July 2013.
- [19] J. W. Simpson-Porco, Q. Shafiee, F. Dörfler, J. C. Vasquez, J. M. Guerrero, and F. Bullo, "Secondary frequency and voltage control of islanded microgrids via distributed averaging," *IEEE Transactions on Industrial Electronics*, vol. 62, pp. 7025–7038, Nov 2015.
- [20] S. Trip, M. Bürger, and C. D. Persis, "An internal model approach to (optimal) frequency regulation in power grids with time-varying voltages," *Automatica*, vol. 64, pp. 240 – 253, 2016.
- [21] J. Simpson-Porco, *Distributed Control of Inverter-Based Power Grids*. PhD thesis, University of California Santa Barbara, 2015.
- [22] W. H. Haemers, "Interlacing eigenvalues and graphs," *Linear Algebra and its applications*, vol. 226, pp. 593–616, 1995.
- [23] I. Lukovits, S. Nikolic, and N. Trinajstić, "Resistance distance in regular graphs," *International Journal of Quantum Chemistry*, vol. 71, pp. 217–225, 1999.
- [24] A. Ghosh, S. Boyd, and A. Saberi, "Minimizing effective resistance of a graph," *SIAM Review*, vol. 50, no. 1, pp. 37–66, 2008.
- [25] I. Gutman and B. Mohar, "The quasi-Wiener and the Kirchhoff indices coincide," *Journal of Chemical Information and Computer Sciences*, vol. 36, no. 5, pp. 982–985, 1996.
- [26] P. G. Doyle and J. I. Snell, "Random walks and electric networks," *American Mathematical Monthly*, vol. 94, no. January, p. 202, 2000.
- [27] P. Barooah and J. P. Hespanha, "Estimation on graphs from relative measurements," *IEEE Control Systems*, vol. 27, pp. 57–74, Aug 2007.
- [28] T. W. Grunberg and D. F. Gayme, "Performance measures for linear oscillator networks over arbitrary graphs," *Preprint*, 2016.
- [29] M. Siami and N. Motee, "Fundamental limits and tradeoffs on disturbance propagation in linear dynamical networks," *IEEE Transactions on Automatic Control*, 2016. to appear.
- [30] B. Bamieh, M. R. Jovanovic, P. Mitra, and S. Patterson, "Coherence in large-scale networks: Dimension-dependent limitations of local feedback," *IEEE Transactions on Automatic Control*, vol. 57, no. 9, pp. 2235–2249, 2012.